Buckling characterization of vertical ZnO nanowires using nanoindentation

Liang-Wen Ji[a)]
Institute of Electro-Optical and Materials Science, National Formosa University, Yunlin 632, Taiwan, Republic of China

Sheng-Joue Young
Institute of Microelectronics, National Cheng Kung University, Tainan 701, Taiwan, Republic of China and Department of Electrical Engineering, National Cheng Kung University, Tainan 701, Taiwan, Republic of China

Te-Hua Fang and Chien-Hung Liu
Institute of Electro-Optical and Materials Science, National Formosa University, Yunlin 632, Taiwan, Republic of China

(Received 3 August 2006; accepted 11 December 2006; published online 17 January 2007)

Nanomechanical characterization of vertical well-aligned single-crystal ZnO nanowires on ZnO:Ga/glass templates was performed by nanoindentation technique. The buckling loads were found to be 1465 and 215 μN for the ZnO nanowires of 100 and 30 nm diameters, respectively. Furthermore, the buckling energies for the ZnO nanowires of 100 and 30 nm diameters were 3.62×10^{-10} and 3.69×10^{-11} J, respectively. Based on the Euler buckling model, Young's modulus of the individual ZnO nanowire has been derived from two possible modes in this work. © *2007 American Institute of Physics*. [DOI: 10.1063/1.2431785]

One-dimensional (1D) materials such as nanowires (NWs), nanobelts, and nanorods have attracted considerable interest in recent years.[1–3] They present the utmost challenge to semiconductor technology, making possible fascinating novel devices. These 1D materials have been demonstrated to exhibit superior electrical, optical, mechanical, and thermal properties, and can be used as nanoscale interconnects, active components of optical electronic devices, and nanoelectromechanical systems. However, it is important to understand the mechanical characteristics of these nanowires prior to any feasible applications. For example, mechanical properties of carbon nanotubes have been extensively studied by tensile loading, bending, and buckling.[2,3]

1D oxide systems such as SnO_2, SiO_2, GeO_2, indium tin oxide, Al_2O_3, and ZnO nanowires have also attracted much attention in recent years.[4–12] Among them, ZnO is a *n* type direct-gap semiconductor with a large exciton binding energy of 60 meV and wide band gap energy of 3.37 eV at room temperature. Hence, ZnO is regarded as a promising photonic material.[13] However, only few reports on the mechanical properties of ZnO nanowires can be found in the literature.[4–8] In this work, the buckling instabilities in vertical ZnO NWs have been characterized by nanoindentation tests. Based on Euler buckling model, we also estimated Young's modulus (elastic modulus) of individual NW.

The ZnO NWs used in this study were grown on ZnO:Ga/glass templates, the synthesis of NWs was performed by a modified self-catalyzed vapor-liquid-solid method without any metal catalyst.[12] Detailed growth procedures can be found elsewhere.[9,10] The photoluminescence (PL) and x-ray diffraction (XRD) were then used to characterize the optical and crystallographic properties of the as-grown ZnO NWs. Surface morphologies of samples and size distribution of the NWs were characterized by a LEO 1530 field-emission scanning electron microscope (FESEM), operated at 5 keV. The investigation on the buckling behavior of the NWs was performed by means of a Hysitron nanoindentation system. Uniaxial compression on the exposed NWs was accomplished with a diamond indenter of 2 μm diameter.

The FESEM images of the as-grown ZnO NWs in samples A and B were shown in Fig. 1(a) and 1(b). We found the typical diameter, length, and density of the ZnO NWs in sample A were approximately 100 nm, 2000 nm, and 8.2×10^{9} cm^{-2} while the ones of sample B were estimated to be 30 nm, 800 nm, and 1.2×10^{10} cm^{-2}, respectively. Note that we can tune the oxygen stream during NW growth to obtain the different size of ZnO NWs. It was found that these ZnO NWs were distributed uniformly across the entire substrate and the tops of these NWs were hexagonal with the *c* axis perpendicular to the substrate surface.[12] As shown in Fig. 1(a), the FESEM image reveals that some wires are stuck together for the 100-nm-diameter wires. For the 30-nm-diameter wires, the same phenomenon is observed, and the wires are also bending and not perfectly straight, as shown in Fig. 1(b). The stuck wires will cause smaller displacement than the single vertical wires under the same load-

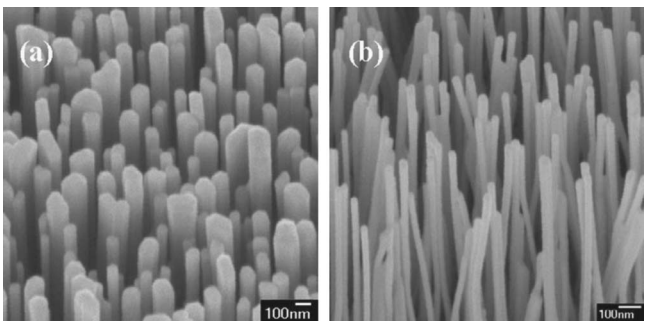

FIG. 1. FESEM images of (a) sample A with the 100-nm-diameter ZnO NWs, and (b) sample B with the 30-nm-diameter ones.

[a)]Author to whom correspondence should be addressed; electronic mail: lwji@seed.net.tw and lwji@nfu.edu.tw

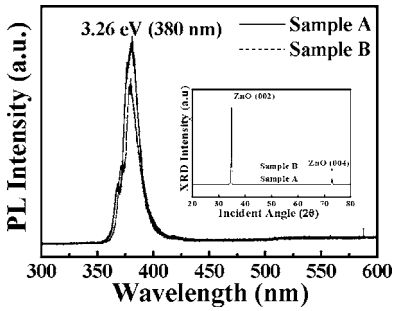

FIG. 2. Room temperature PL spectra of the as-grown ZnO NWs (samples A and B). Inset exhibits XRD spectra for samples A and B.

ing force. Furthermore, it will also result in higher critical buckling loads and Young's modulus of the NW samples. From x-ray diffraction and photoluminescence measurements (Fig. 2), it was found that the ZnO nanowires were preferred oriented in the (002) *c* axis direction with good crystal quality.

Samples A and B with the vertical ZnO NWs of 100 and 30 nm diameters were used in the nanoindentation tests. The NWs were loaded to a prescribed force and then unloaded in a force-controlled mode. Because each test was destructive in nature, several tests on different areas of the sample were conducted to check for repeatability. As shown in the inset of Fig. 3, it can be seen that the distorted ZnO NWs (sample B) appeared after the nanoindentation experiments. Note that the opening angle of the conical indenter is estimated to 70°. We predict that the effect of opening angle could result in an increase of larger contact areas and higher critical buckling loads for NWs; therefore Young's moduli will be evaluated slightly higher.

It is well known that the behavior of an ideal column and/or nanowire compressed by an axial load P can be summarized as follows: (1) if $P<P_{cr}$, the column is in *stable* equilibrium in the straight position; (2) if $P=P_{cr}$, the column is in a *neutral* equilibrium in either the straight or a slightly bent position; and (3) if $P>P_{cr}$, the column is in *unstable* equilibrium in the straight position and will buckle under the slightest disturbance. Such a type of buckling is called Euler buckling.[14] Figure 3 shows load-displacement curves of the ZnO NW samples, in which each plot represents a loading-unloading cycle. The loading portion consists of three stages: an initial increase ($P<P_{cr}$), followed by a sudden drop in the slope and the curve becomes flat ($P=P_{cr}$), and a third stage comprising an increasing load ($P>P_{cr}$). Where sample B shows less contact force than sample A in the initial elastic regions of the load-displacement curves, the behavior of buckling instability is observed in the flat regions. Hence, the individual ZnO NW in this work can be regarded as an ideal column. The collapse force is 1465 μN for sample A, whereas it is 215 μN for sample B, as shown in Fig. 3. The critical buckling loads of the ZnO NWs are therefore found to be 1465 and 215 μN for samples A and B, respectively. Furthermore, the buckling energies were 3.62×10^{-10} and 3.69×10^{-11} J for samples A and B, respectively.

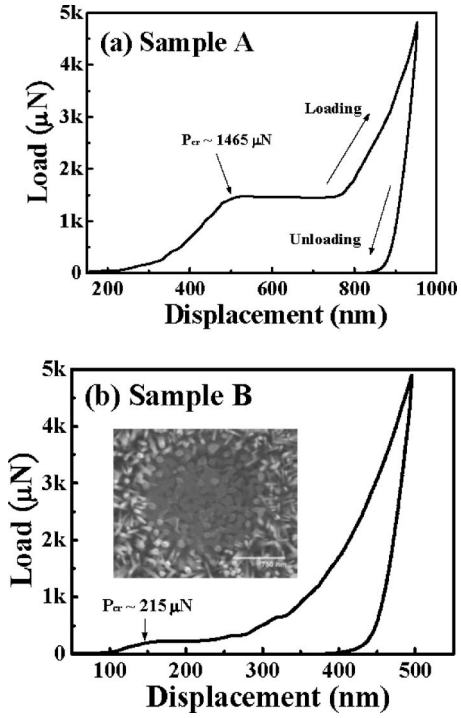

FIG. 3. Force vs displacement curve of sample A (a) and sample B (b). Inset shows a FESEM image of the buckled ZnO NWs (sample B) in top view.

TABLE I. Critical stress, critical buckling strain, and Young's modulus of the ZnO NWs.

Sample description (length: L, diameter: D)	σ_{cr} (MPa)	K	ε_{cr} (%)	E (GPa)
A (ZnO NWs) $L=2000$ nm, $D=100$ nm	723	0.5	0.62	117
	723	0.7	0.32	229
B (ZnO NWs) $L=800$ nm, $D=30$ nm	806	0.5	0.35	232
	806	0.7	0.18	454
Single-crystal bulk wurtzite ZnO				111.2[a]

[a]Reference 15.

By the FESEM images of the buckled ZnO NWs in top view, as shown in the inset of Fig. 3, we can easily estimate the average critical buckling loads of individual ZnO NW for samples A and B at about 5.68 and 0.57 μN, respectively. This value is important in determining Young's modulus of a single ZnO NW.

The critical load for an ideal elastic column is often called the Euler load and is given by $P_{cr}=\pi^2EI/L_e^2$, where E is Young's modulus and the moment of inertia is $I=\pi R^4/4$ for the column (vertical ZnO NW). The effective length L_e is expressed in terms of an effective-length factor K: $L_e=KL$, where L is the actual length of the column. The buckling behavior of ZnO NWs in this work can be approached by two possible conditions as follows: (1) $K=0.5$, a nanocolumn with both ends fixed against rotation is called a fixed-fixed column, where $P_{cr}=4\pi^2EI/L^2$; (2) $K=0.7$, a nanocolumn fixed at the base and pinned at the top is called a fixed-pinned column, where $P_{cr}=2.046\pi^2EI/L^2$. For an Euler buckling column, the critical buckling strain is given by $\varepsilon_{cr}=\sigma_{cr}/E$, where critical buckling stress $\sigma_{cr}=P_{cr}/A$.[14]

As shown in Table I, we can estimate critical stress (σ_{cr}), critical buckling strain (ε_{cr}), and Young's modulus (E) of ZnO NWs by critical buckling load of individual ZnO NW. It should be noted that the value of Young's modulus for single-crystal ZnO bulk is 111.2 GPa,[15] and smaller than the values of ZnO NWs. Based on Euler buckling, it was found that Young's modulus of ZnO NWs increases with decreasing diameter whether we evaluate the ones by fixed-fixed

column ($K=0.5$) or fixed-pinned column ($K=0.7$) mode. These results correspond with the work of molecular dynamics simulations performed by Kulkarni *et al.*,[6] as well as the experimental revelation of Chen *et al.*[7] This behavior can be attributed to high compressive internal stress levels resulting from the surface stress and high surface-to-volume ratios at the nanoscale.[6,7] In other words, because our experimental NWs are high quality single crystals with few defects, it is expected that such a phenomenon of size dependence may originate from surface modification of NWs, as the surface effect becomes significant due to the large surface-to-volume ratio.

In summary, we report the experimental observations of buckling instabilities of vertical well-aligned single-crystal ZnO nanowires prepared on ZnO:Ga/glass templates. The critical buckling loads of the ZnO NWs are found to be 1465 and 215 μN for samples A (100 nm diameter) and B (30 nm diameter), respectively. Furthermore, the buckling energy was 3.62×10^{-10} and 3.69×10^{-11} J for samples A and B, respectively. Euler buckling model can be employed in evaluating Young's modulus (E) and the critical buckling strain (ε_{cr}) of individual ZnO NW.

This work was supported by National Science Council of Taiwan under Contract No. NSC-95-2221-E-150-077-MY3. The authors would like to thank the Advanced Optoelectronic Technology Center, National Cheng Kung University, Taiwan for the support through equipment and cooperation.

[1] L. W. Ji, T. H. Fang, S. C. Hung, Y. K. Su, S. J. Chang, and R. W. Chuang, J. Vac. Sci. Technol. B **23**, 2496 (2005).
[2] P. Poncharal, Z. L. Wang, D. Ugarte, and W. A. de Heer, Science **283**, 1513 (1999).
[3] M. F. Yu, O. Lourie, M. J. Dyer, K. Moloni, T. F. Kelly, and R. S. Ruoff, Science **287**, 637 (2000).
[4] H. Saitoh, Y. Namioka, H. Sugata, and S. Ohshio, Jpn. J. Appl. Phys., Part 1 **40**, 6024 (2001).
[5] S. X. Mao, M. H. Zhao, and Z. L. Wang, Appl. Phys. Lett. **83**, 993 (2003).
[6] A. J. Kulkarni, M. Zhou, and F. J. Ke, Nanotechnology **16**, 2749 (2005).
[7] C. Q. Chen, Y. Shi, Y. S. Zhang, J. Zhu, and Y. J. Yan, Phys. Rev. Lett. **96**, 075505 (2006).
[8] Z. L. Wang and J. H. Song, Science **312**, 242 (2006).
[9] V. Valcarcel, A. Souto, and F. Guitian, Adv. Mater. (Weinheim, Ger.) **10**, 138 (1998).
[10] Z. W. Pan, Z. R. Dai, and Z. L. Wang, Science **291**, 1947 (2001).
[11] Z. R. Dai, Z. W. Pan, and Z. L. Wang, Adv. Funct. Mater. **13**, 9 (2003).
[12] C. L. Hsu, S. J. Chang, H. C. Hung, Y. R. Lin, C. J. Huang, Y. K. Tseng, and I. C. Chen, IEEE Trans. Nanotechnol. **4**, 649 (2005).
[13] Z. X. Mei, X. L. Du, Y. Wang, M. J. Ying, Z. Q. Zeng, H. Zheng, J. F. Jia, Q. K. Xue, and Z. Zhang, Appl. Phys. Lett. **86**, 112111 (2005).
[14] S. P. Timoshenko and J. M. Gere, *Theory of Elastic Stability* (McGraw-Hill, New York, 1961), p. 46.
[15] S. O. Kucheyev, J. E. Bradby, J. S. Williams, C. Jagadish, and M. V. Swain, Appl. Phys. Lett. **80**, 956 (2002).